

Electronic spin transport and spin precession in single graphene layers at room temperature

Authors: Nikolaos Tombros, Csaba Jozsa, Mihaita Popinciuc, Harry T. Jonkman, Bart J. van Wees,

arXiv:0706.1948, Nature 448, 571-574 (2007).

Recommended with a Commentary by Roland Kawakami, University of California, Riverside

Carbon based systems are attractive for spin-based electronics due to the low spin-orbit coupling and low hyperfine coupling which should lead to long spin coherence times. The low spin-orbit coupling is due to the low atomic number of carbon, and the low hyperfine coupling is due to the fact that ^{12}C (98.9% abundance) has zero nuclear spin.

The past year has witnessed numerous reports of spin injection and transport in ultrathin graphite (i.e. single-layer and multi-layer graphene) [1-6]. Among this group of papers, the work by van Wees stands out because it demonstrates both spin injection and precession at room temperature.

I will first summarize the principal findings of the paper and then present what in my view are the interesting issues that this and similar investigations raise.

Key Figures of the Paper

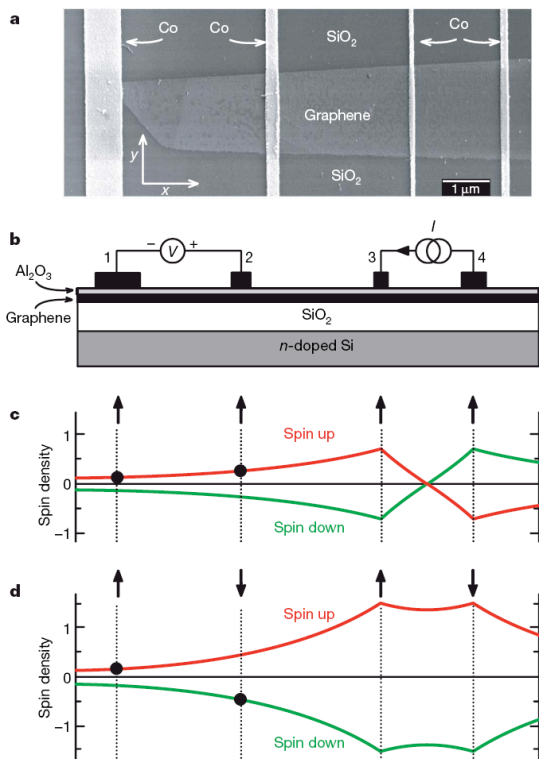


Figure 1 of paper: Sample geometry and spin density profile

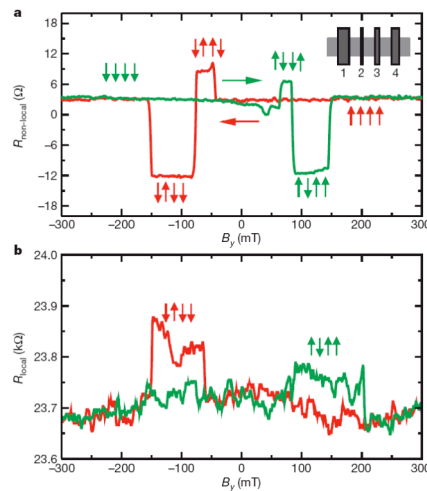


Figure 2 of paper: (a) Non-local signal. (b) Local magnetoresistance.

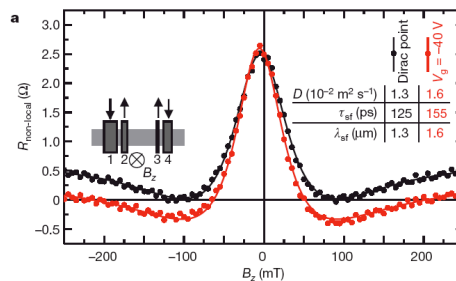


Figure 4a of paper: Electron spin precession induced by out-of-plane B field.

Summary of the paper

As shown in Fig. 1, the device consists of a graphene sheet covered by an Al_2O_3 tunnel barrier and multiple Co electrodes on top. The widths of the Co electrodes are different so that the magnetization reversals occur at distinct magnetic fields due to the magnetic shape anisotropy (i.e. magnetostatic energy). This geometry enables the “non-local” spin injection measurement and the Hanle effect measurement, which were discussed in detail in my last journal club entry and have been applied previously to measure spin injection in metals [7] and semiconductors [8]. Referring to Fig. 1, spin-polarized carriers are injected from Co electrode #3 into the graphene layer. The charge current flows to the right toward electrode #4, but due to spin diffusion, the spin-polarization will flow to the left toward electrodes #1 and #2 even though there is no net charge flow in that direction. The arrival of spin to electrode #2 is detected by measuring the voltage between electrodes #2 and #1. Due to the a spin-dependent chemical potential and the spin-dependent density of states of the Co electrode, the voltage signal will be positive if the magnetizations of Co #2 and Co #3 are parallel, and the voltage signal will be negative if their magnetizations are antiparallel (Figure 1c, d). Usually the electrodes #1 and #4 are non-magnetic, but making all the electrodes of the same material makes the fabrication simpler and there are only minor differences in the non-local magnetoresistance data.

Referring to the main data in Fig. 2a, the non-local resistance (defined as $R_{\text{non-local}} = V_{12}/I_{34}$) is measured as a function of magnetic field which is applied in-plane and along the long axes of the Co electrodes. The hysteretic switching of $R_{\text{non-local}}$ is related to the relative magnetizations of the four Co electrodes. The two primary values for $R_{\text{non-local}}$ are $+3\Omega$ and -12Ω , which correspond to the parallel and antiparallel magnetization alignments of Co #2 and Co #3. The magnitude of the spin signal is $\Delta R_{\text{non-local}} = 15 \Omega$ in this case. The other small jumps are related to switching of the other two electrodes (#1 and #4), and are not so important.

Out of five devices exhibiting non-local spin signal, one of these has shown a “local” spin signal, which is obtained by re-wiring the device and measuring the resistance between Co #2 and Co #3 during the magnetic field sweep ($R_{\text{local}} = V_{23}/I_{23}$). This shown in Figure 2b and the magnetoresistance is $\Delta R/R \approx 0.1\text{k}\Omega/23.7\text{k}\Omega = 0.4\%$.

Application of a gate voltage (via silicon backgate) can make the carrier type to be electrons or holes and the carrier density can be tuned. The spin signal ($\Delta R_{\text{non-local}}$) exhibits a dependence on gate voltage, V_g . At the Dirac point which is the boundary between the electron and hole regime ($V_g = 19 \text{ V}$ in this device), the spin signal is reduced to about 65% of its value at $V_g = -40 \text{ V}$ (Fig. 3 of paper, not shown here).

Finally, the measurement of electron spin precession is performed by applying an out-of-plane magnetic field (Fig. 4). In zero magnetic field, there is no precession and the spin signal is maximized. With increasing field, the spin signal experiences damped oscillations due to the spin precession. The damped shape occurs because the spin polarization under the detection electrode (Co #2) is the polarization of precessing spins averaged over a broad range of arrival times (the transport is diffusion, not drift). The shape of the curve is given by:

$$\int_0^{\infty} \frac{1}{\sqrt{4\pi Dt}} \exp\left(-\frac{L^2}{4Dt}\right) \exp\left(-\frac{t}{\tau}\right) \cos(g\mu_B H_{\perp} t / \hbar) dt$$
, where D is the diffusion constant, τ is the spin lifetime, L is the distance between electrodes #2 and #3, H_{\perp} is the out-of-plane field. Fitting the data gives values of spin lifetime τ , which is on the order of 150 ps. The two curves in Figure 4 are for the system at the Dirac point ($V_g = 19 \text{ V}$) and at $V_g = -40 \text{ V}$.

Some Interesting Issues

1) This is the first very clear demonstration of spin transport in graphene. The spin transport characteristics are good with signals at room temperature and respectable spin diffusion lengths of $1.5 - 2 \mu\text{m}$. In contrast, lateral spin transport in metals exhibits non-local signals at room temperature and has spin diffusion lengths below 500 nm [9]. In GaAs and Si, the spin signals are only observed below room temperature [8,10]. Thus graphene is right now perhaps the best spin transport material at room temperature. The spin lifetimes, however, are only $\sim 150 \text{ ps}$ at room temperature. It is hoped that cleaner samples could make these lifetimes longer. Theoretical studies of spin-lifetimes in ideal structures would be valuable, as would experimental studies of spin relaxation in graphite via pulsed ESR measurements.

2) The magnitude of the non-local spin signal is $\sim 15 \Omega$, which is much larger than in the similar spin signals in metallic systems which are $\sim 10 \text{ m}\Omega$ [7]. This could be understood by considering the equation given in the paper: $R_{\text{nl}} = (P^2 \lambda_{\text{sf}} / 2W\sigma_{2\text{D}}) \exp(-L/\lambda_{\text{sf}})$, where $\sigma_{2\text{D}}$ is the 2D conductivity, W is the width of the graphene, P is the injected polarization, and λ_{sf} is the spin diffusion length. In 3D metals, the $\sigma_{2\text{D}}$ is replaced by $\sigma_{3\text{D}}d$ (d is the thickness), which is typically much larger and therefore generates a smaller non-local spin signal R_{nl} .

3) This work shows both the non-local spin signal (Figure 2a) and the corresponding local spin signal (Figure 2b). This is actually rather unusual. Four out of five devices exhibiting non-local signal do not exhibit any local signal. Only one out of the five devices exhibits the local signal, and the magnitude is only 0.4% magnetoresistance. From this, one could conclude that the non-local measurement is more sensitive than the local measurement in detecting spin. In some of our unpublished work, we also are able to obtain non-local signals in devices that do not show local spin signals, consistent with van Wees's results. Of the published work of spin injection into graphene, some are based on non-local measurements [2,3,5] while others are based on local magnetoresistance measurements [1,4,6].

4) Is the presence of the tunnel barrier needed for spin injection into graphene? In some works [3,6], the use of a tunnel barrier is put forward as a necessary ingredient to avoid the conductivity mismatch problem, which states that spin injection from a ferromagnetic metal into a material with significantly lower conductivity (i.e. semiconductor) is very inefficient unless tunnel barriers are employed [11-13]. On the other hand, some other groups achieve spin injection into graphene without the use of a tunnel barrier, although it is possible that some devices might benefit from "dirty" contacts. More experimental and theoretical studies are needed to address the role of tunnel barriers on the spin injection into graphene and graphite. On the experimental side, the materials issues are significant. In the van Wees paper, they make the Al_2O_3 tunnel barrier by depositing Al at 77K to reduce pinhole formation. In our own studies using MgO barriers [6], a major challenge is to achieve barriers free of pinholes.

5) What are the unique spin-dependent properties of graphene? The low spin-orbit coupling and low hyperfine coupling already make graphene and graphite attractive materials for spin transport. But in addition to this, what are the possible special spin-dependent properties of graphene due to its unusual 2D, relativistic-like band structure? For example, it is predicted that graphene should possess ferromagnetic order under the appropriate conditions [14,15]. How would such properties influence spin-polarized transport?

- [1] E. W. Hill, A. K. Geim, K. S. Novoselov, F. Schedin and P. Blake, "Graphene Spin Valve Devices", *IEEE Trans. Magn.* **42**, 2694-2696 (2006).
- [2] M. Ohishi, M. Shiraishi, R. Nouchi, T. Nozaki, T. Shinjo and Y. Suzuki, "Spin injection into a graphene thin film at room temperature", *Japanese Journal of Applied Physics* **46**, L605-L607 (2007).
- [3] N. Tombros, C. Jozsa, M. Popinciuc, H. T. Jonkman and B. J. Van Wees, "Electronic spin transport and spin precession in single graphene layers at room temperature", *Nature* **448**, 571-574 (2007).
- [4] M. Nishioka and A. M. Goldman, "Spin Transport Through Multilayer Graphene", *Appl. Phys. Lett.* **90**, 252505 (2007).
- [5] S. Cho, Y.-F. Chen and M. S. Fuhrer, "Gate-tunable graphene spin valve", *Appl. Phys. Lett.* **91**, 123105 (2007).
- [6] W. H. Wang, K. Pi, Y. Li, Y. F. Chiang, P. Wei, J. Shi and R. K. Kawakami, "Magnetotransport properties of mesoscopic graphite spin valves", *Phys Rev. B (Rapid Comm.)* **77**, 020402 (2008).
- [7] F. J. Jedema, H. B. Heersche, A. T. Filip, J. J. A. Baselmans and B. J. van Wees, "Electrical Detection of Spin Precession in a Metallic Mesoscopic Spin Valve", *Nature* **416**, 713-716 (2001).
- [8] X. Lou, C. Adelman, S. A. Crooker, E. S. Garlid, J. Zhang, K. S. Madhukar Reddy, S. D. Flexner, C. J. Palmstrom and P. A. Crowell, "Electrical Detection of Spin Transport in Lateral Ferromagnet-Semiconductor Devices", *Nature Physics* **3**, 197-202 (2007).
- [9] S. O. Valenzuela and M. Tinkham, "Spin-polarized tunneling in room-temperature mesoscopic spin valves", *Appl. Phys. Lett.* **85**, 5914-5916 (2004).
- [10] I. Appelbaum, B. Huang and D. J. Monsma, "Electronic Measurement and Control of Spin Transport in Silicon", *Nature* **447**, 295-298 (2007).
- [11] G. Schmidt, D. Ferrand, L. W. Molenkamp, A. T. Filip and B. J. van Wees, "Fundamental Obstacle for Electrical Spin Injection from a Ferromagnetic Metal into a Diffusive Semiconductor", *Phys. Rev. B (Rapid Communications)* **62**, 4790-4793 (2000).
- [12] E. I. Rashba, "Theory of electrical spin injection: Tunnel contacts as a solution of the conductivity mismatch problem", *Phys. Rev. B (Rapid Communications)* **62**, 16267-16270 (2000).
- [13] A. Fert and H. Jaffres, "Conditions for efficient spin injection from a ferromagnetic metal into a semiconductor", *Phys. Rev. B* **64**, 184420 (2001).
- [14] N. M. R. Peres, F. Guinea and A. H. Castro Neto, "Coulomb Interactions and Ferromagnetism in Pure and Doped Graphene", *Phys. Rev. B* **72**, 174406 (2005).
- [15] Y.-W. Son, M. L. Cohen and S. G. Louie, "Half-metallic graphene nanoribbons", *Nature* **444**, 347-349 (2006).